doi:10.1111/evo.13786

Anatomical diversification of a skeletal novelty in bat feet

Kathryn E. Stanchak,[1,2] Jessica H. Arbour,[1] and Sharlene E. Santana[1]

[1]*Department of Biology and Burke Museum of Natural History and Culture, University of Washington, Seattle, Washington 98195*

[2]*E-mail: stanchak@uw.edu*

Received December 21, 2018
Accepted May 18, 2019

Neomorphic, membrane-associated skeletal rods are found in disparate vertebrate lineages, but their evolution is poorly understood. Here we show that one of these elements—the calcar of bats (Chiroptera)—is a skeletal novelty that has anatomically diversified. Comparisons of evolutionary models of calcar length and corresponding disparity-through-time analyses indicate that the calcar diversified early in the evolutionary history of Chiroptera, as bats phylogenetically diversified after evolving the capacity for flight. This interspecific variation in calcar length and its relative proportion to tibia and forearm length is of functional relevance to flight-related behaviors. We also find that the calcar varies in its tissue composition among bats, which might affect its response to mechanical loading. We confirm the presence of a synovial joint at the articulation between the calcar and the calcaneus in some species, which suggests the calcar has a kinematic functional role. Collectively, this functionally relevant variation suggests that adaptive advantages provided by the calcar led to its anatomical diversification. Our results demonstrate that novel skeletal additions can become integrated into vertebrate body plans and subsequently evolve into a variety of forms, potentially impacting clade diversification by expanding the available morphological space into which organisms can evolve.

KEY WORDS: **Chiroptera, early burst, evolutionary novelty, flight, morphology, neomorphism.**

In *On the Origin of Species*, Darwin repeatedly argued against the abrupt appearance of novel biological forms by invoking "*Natura non facit saltum*" (Darwin 1859; annotations by Costa in Darwin and Costa 2009). Whether—or how often—novelties emerge and significantly influence the course of evolution (a proverbial leap of nature) immediately became a subject of debate among both Darwin's critics and supporters (Huxley 1860), and this debate has persisted through the Modern Synthesis era to the present (e.g., Simpson 1944; Berry 1985; Orr and Coyne 1992; Wagner 2014; Erwin 2015; Jablonski 2017). It remains unclear how impactful anatomical novelty (by any definition, see Moczek 2008; Pigliucci 2008; Peterson and Müller 2013; Wagner 2014) is on the evolutionary trajectory of a clade. This is particularly true of discrete structures that lack obvious homologous counterparts in predecessor taxa. Although the loss, repetition, or extreme modification of anatomical features are recognized as potential mechanisms of functional and phylogenetic diversification (e.g., in vertebrates, the loss of limbs and repetition of the axial skeleton in snakes [Cohn and Tickle 1999; Martill et al. 2015] or the modification of developing skin placodes in the evolution of feathers [Musser et al. 2015; Di-Poï and Milinkovitch 2016]), the paleontological and neontological records of evolution still contain neomorphic anatomical elements that are not well understood in terms of both their origin and evolution (e.g., in vertebrates; Hall 2015).

Recent fossil discoveries have raised interest in one specific type of novel skeletal structure: the "styliform" elements of amniotes that use membranes to glide or fly (Fig. 1). This group of skeletal elements comprises the calcar of bats (Schutt and Simmons 1998), the styliform cartilages of gliding rodents and one marsupial (Johnson-Murray 1987; Jackson 2012; Coster et al. 2015; Kawashima et al. 2017), the pteroid of pterosaurs (Bennett 2007), and was recently expanded to include the styliform element of *Yi qi*, a maniraptoran theropod dinosaur (Xu et al. 2015), and the calcar of *Maiopatagium furculiferum*, a haramiyid mammaliaform (Meng et al. 2017). Because these skeletal rods are now known from disparate amniote lineages,

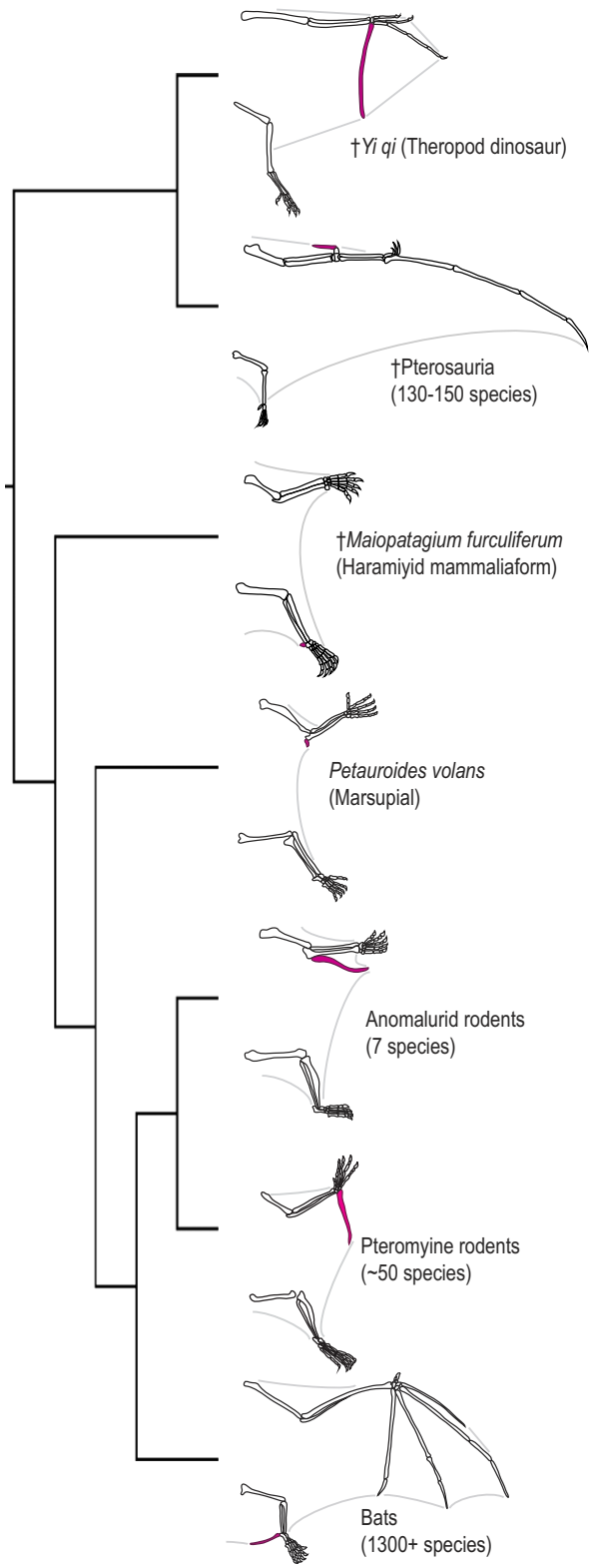

Figure 1. **Neomorphic skeletal rods have evolved multiple times in vertebrates with gliding or flying membranes. These structures are indicated in pink in the schematic drawings. Drawings based on Johnson-Murray 1987, Bennett 2007, Jackson 2012, Witton 2013, Coster et al. 2015, Xu et al. 2015, Kawashima et al. 2017, Meng et al. 2017.**

they seem less like evolutionary oddities than consequential skeletal novelties characteristic of the skin membranes of volant body plans. The literature on most of these appendicular ossicles associated with skin membranes (Vickaryous and Olson 2007) is limited to osteological descriptions (e.g., citations above), so much is still unknown about their function, origin, and diversification. The pterosaur pteroid has been the focus of several studies (summarized in Witton 2013), but although the Pterosauria comprises a taxonomically diverse clade in which to explore pteroid variation, the lack of extant successors in the lineage restricts detailed anatomical and functional studies. In contrast, another of these neomorphic styliform elements—the bat calcar—is widespread across extant bats, making it an ideal model system for gaining a better understanding of the evolution of membrane-bound skeletal rods, and more generally, the evolution of neomorphic skeletal elements.

Bats (Chiroptera) are systematically, morphologically, and ecologically diverse (Kunz and Fenton 2005; Simmons 2005; Fenton and Simmons 2015). The calcar articulates with the calcaneus in the bat ankle and extends into the membrane that spans between the two hindlimbs (Vaughan 1970; Fig. 1). It abruptly appears in the early bat fossil record (*Onychonycteris finneyi*, Onychonycteridae, Green River Formation, WY, USA; ~52.5 Ma; Simmons et al. 2008) and, based on its ubiquity among extant bats, seems to have become fixed within the bat wing structure. In the terminology of evolutionary novelty, the calcar might be considered both a "novel character identity" or "Type I novelty" under the typology of Wagner (2014) and a "discrete new element added to an existing body plan" or "Type II novelty" under the typology of Müller (2010). In addition, it meets Hall's (2015) definition of neomorphs, which "*seem to appear out of nowhere, de novo,* but are present in most if not all individuals of a species." The calcar is typically described as a bony or cartilaginous element, although histological studies to date have confirmed only the presence of cartilaginous tissue with varying levels of mineralization (Schutt and Simmons 1998; Adams and Thibault 1999; Czech et al. 2008; Stanchak and Santana 2018). Because bats are morphologically diverse and cartilage can be a precursor of bone, it has been hypothesized that the calcars of some bat species might be composed of bony tissue (Adams and Thibault 1999).

The specific functions of the calcar are unknown, but it is generally described as providing support for the hindlimb membrane (Vaughan 1970). However, bat hindlimbs have functions other than flight (e.g., roosting, and in some bats, prey capture; Novick and Dale 1971), so calcars may also take on different functions in species that vary ecologically. Functionally diverse calcars should exhibit anatomical divergence based on differing functional requirements. For instance, in *Myotis*, long calcars were found to be associated with a trawling foraging strategy (Fenton and Bogdanowicz 2002), and muscles associated with the calcar

were found to vary anatomically in three species with different flight and foraging strategies (Stanchak and Santana 2018).

In all animal clades with styliform elements, including bats, the evolution of membrane-bound limbs and a new locomotor mode (flight or gliding) allowed entry into new ecological space: the aerosphere. The bat fossil record demonstrates early taxonomic diversification coupled with a rapid expansion of their geographic distribution (Smith et al. 2012). Based on its presence in some of the earliest bat fossils (Simmons and Geisler 1998; Simmons et al. 2008), the calcar may be part of the suite of adaptations that allowed bats to functionally and ecologically radiate into varied niches after their initial invasion of the aerosphere. If so, we predict that (1) bat calcars will be morphologically diverse in trait parameters that theoretically affect function, and (2) calcar morphological diversification will reflect the rapid early diversification of Chiroptera, as suggested by the fossil record.

In this article, we assess and describe the anatomical diversification of the calcar across the radiation of bats to test the predictions outlined above. We integrate a variety of methods to analyze calcar anatomy across a broad sample of bat species spanning diverse ecologies. First, we examine variation in the length of the calcar across Chiroptera and test different models of calcar evolution to reveal the macroevolutionary patterns and potential underlying processes that characterize calcar diversification. Then, we more closely investigate the anatomical diversity of the calcar with micro-Computed Tomography (μCT) scans to assess its status as a novel skeletal addition rather than another type of skeletal modification (e.g., a repeated tarsal element), and we integrate data from both μCT scans and histological sections to test the hypothesis that the calcar has histologically diversified. Finally, we combine gross dissections and diffusible iodine-based contrast-enhanced μCT (diceCT; Gignac et al. 2016) for the visualization of soft tissue to evaluate whether the calcars of all bats are homologous. These detailed anatomical studies inform the interpretations of the macroevolutionary modeling, allowing us to rigorously assess the scope and scale of bat calcar evolution.

Material and Methods

CALCAR LENGTH MEASUREMENTS AND MACROEVOLUTIONARY ANALYSES

The length of a rod or shaft is one parameter that determines its ability to resist bending under an applied load (Hibbeler 2007). Bat calcars generally take a rod-shaped form, so comparisons of calcar length are informative about the potential functional importance of the calcar across bats. A single observer (KES) made caliper measurements of calcar, tibia, and forearm (i.e., radius) lengths of one to nine fluid-preserved specimens representing 226 species and all recognized families within Chiroptera. In total, the sample included 1396 specimens with an average of six specimens per species. A list of museum specimens is provided as a spreadsheet in the Supporting Information. By measuring intact, fluid-preserved specimens, we ensured that any thin, cartilaginous portions of the calcar were present and measured. We rounded caliper measurements to the nearest 1 mm to reflect imprecision in measuring skeletal features from external examination of intact specimens. Because we based all measurements on external examination of specimens, it is possible that a very small, not externally evident calcar resulted in assigning a value of 0 mm to the calcar length for some individuals (e.g., see Results regarding *Rhinopoma hardwickii*). We did not include fossil bat species in our sample because few postcrania are present in the bat fossil record and the calcars of some extant species are unmineralized, so we would not be able to confirm the absence of a calcar for any bat fossil species.

For each specimen, we calculated the ratio of the calcar length divided by either the tibia or the forearm length and then averaged these ratios across all specimens for a particular species. This allowed us to derive a unitless measure of hidlimb skeletal proportions for comparisons across species. We visualized the calcar-to-tibia length ratio character states on a pruned version of a relatively recent chiropteran phylogeny (Shi and Rabosky 2015) using the "fastAnc" method of the "contMap" function (Felsenstein 1985; Revell 2013) from the *phytools* version 0.6 package (Revell 2012) in R version 3.4.3 (R Core Team 2017; all analyses were performed in the same version of R). We also calculated the residuals of phylogenetic-generalized least squares (pgls) regressions of mean calcar length on mean tibia or mean forearm length assuming a Brownian motion correlation structure using the "phyl.resid" function (Revell 2009, 2010) from the *phytools* version 0.6 R package (Revell 2012). Although the calcar-to-tibia length ratio is more intuitively relevant to calcar biomechanics and function, even beyond its use for size normalization, we used both the tibia and forearm ratios and pgls residuals in subsequent evolutionary analyses so that we could better interpret the effect of variable transformations on our model fits. In addition, we repeated all of the following analyses for datasets excluding the species for which we recorded a calcar length of 0 mm because a calcar was not externally visible on the specimens. We also repeated all of the following analyses using datasets from which we excluded the Old World fruit bats (Pteropodidae) due to their differing calcar anatomy. Pteropodid calcars are described as inserting on the tendon of the gastrocnemius muscle rather than articulating with the calcaneus and are consequently hypothesized to not be homologous to the calcars of other bats (Schutt and Simmons 1998; Kobayashi 2017). All data used in analyses are provided as a spreadsheet in the Supporting Information.

To gain insight on the evolutionary processes that may have led to extant calcar diversity, we fit three models

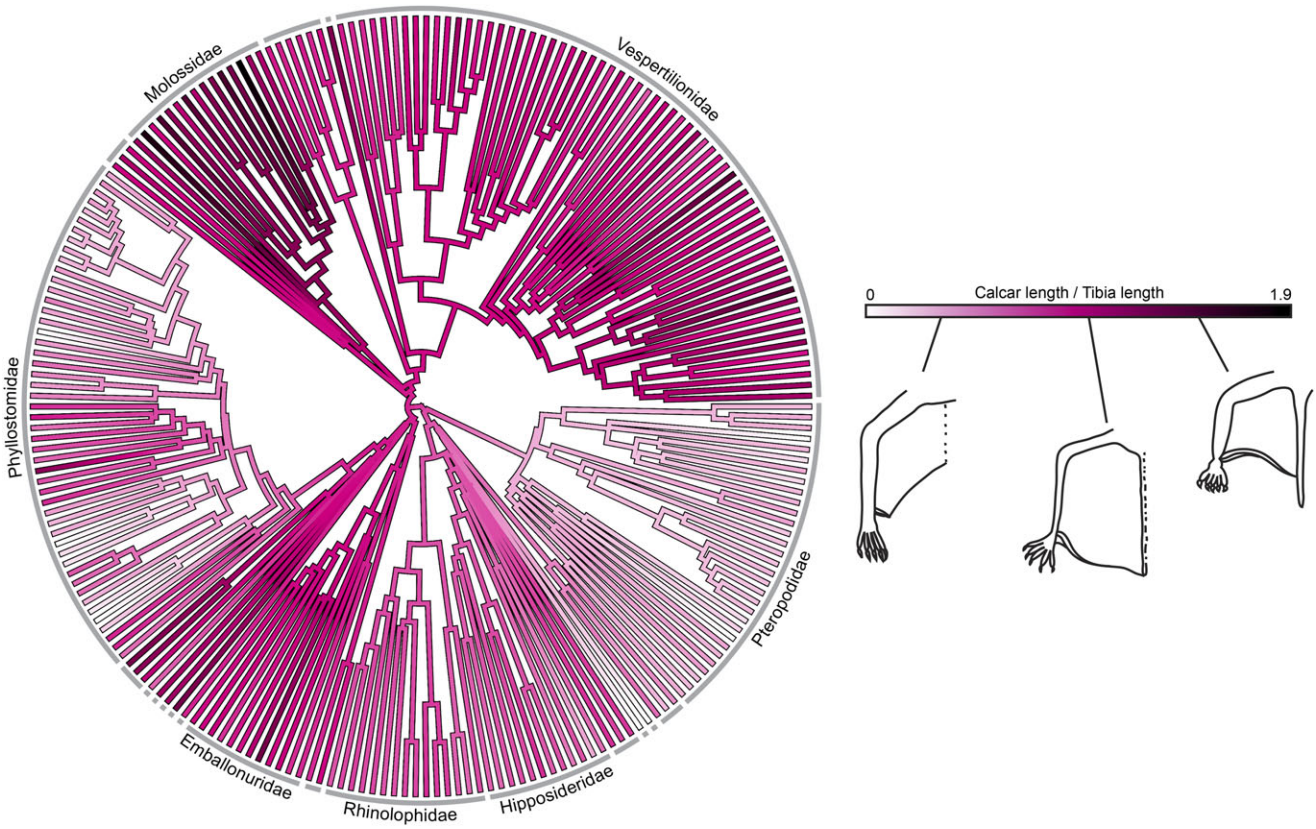

Figure 2. **Relative calcar length varies extensively across Chiroptera. Ratio of calcar length-to-tibia length is plotted on a phylogeny of Chiroptera (Shi and Rabosky 2015). Gray lines around the phylogenetic tree designate bat families; species-rich families are labeled. Schematic drawings on the color scale illustrate representative hindlimb morphologies for different calcar lengths.**

of evolution (Brownian motion, early burst, and single-peak Ornstein–Uhlenbeck) to the calcar length ratios and pgls residuals using the "fitContinuous" function in the *geiger* version 2.0.6 R package (Harmon et al. 2007; Pennell et al. 2014). Brownian motion (BM) models a "random-walk" process in which the variance of a trait increases linearly through time (as defined in evolutionary modeling by the evolutionary rate parameter σ^2). It is often used to test the hypothesis of trait evolution under a drift or other random process (Felsenstein 1973). The early burst (EB) model is used to test a niche-filling hypothesis consistent with an adaptive radiation; the rate at which a trait diversifies decreases with declining ecological opportunity after an initial, rapid "early burst" of diversification (Blomberg et al. 2003; Harmon et al. 2010). The EB model is parameterized by the initial evolutionary rate (σ^2) and a parameter for the exponential change in evolutionary rates through time (a), such that when $a = 0$ the EB model reduces to the BM model and when $a < 0$ evolutionary rates decrease as time progresses (Harmon et al. 2007; Harmon et al. 2010). An Ornstein–Uhlenbeck (OU) process is used to model an evolutionary process in which some restoring force (e.g., selection; parameterized by α) restrains a trait value (θ) through time (Hansen 1997; Butler and King 2004). As implemented here, the model assumes a single optimal trait value that is equal to the root ancestral state of the trait (Harmon et al. 2007; parameterized by z_0 in all models). We compared these three models using small sample size-corrected Akaike weights (w_{AICc}). If the calcar underwent an early morphological diversification as the first bats phylogenetically diversified, we expected to find the highest support for the EB model.

To visualize and quantify the tempo of calcar length evolution, we performed a disparity-through-time analysis using the "dtt" function (Harmon et al. 2003; Slater et al. 2010) from the *geiger* version 2.0.6 R package (Harmon et al. 2007; Pennell et al. 2014). This analysis calculates the mean morphological disparity of each subtree in the pruned phylogeny using the average squared Euclidean distance among all pairs of points. We plotted this curve against a null distribution created by using the same procedure on a set of 1000 simulations across the pruned phylogeny assuming a BM model of evolution of the relative calcar lengths. We used the morphological disparity index (MDI) to quantitatively compare subclade disparity in relative calcar length with the disparity expected under a BM model (Harmon et al. 2003; Slater et al.

2010). We determined the significance of the MDI by the frequency at which a calculated MDI between the dataset and each simulation trial was greater than zero. A negative MDI value indicates that disparity is partitioned more strongly among early divergence events, with more recent subclades each representing only a small portion of the total morphological diversity of the clade than expected under a constant-rate, random walk process (e.g., BM; Harmon et al. 2003; Slater et al. 2010). Positive MDI values may be indicative of selective constraint or increasing evolutionary rates, where each recent subclade is more likely to represent a greater proportion of trait space (López-Fernández et al. 2013). A negative MDI supports a hypothesis of early, rapid morphological diversification prior to a period of relative stasis until the present day (Slater et al. 2010). To more rigorously assess the prediction of early disparification, we also calculated the MDI between the dtt curve and a curve distribution simulated under an EB model of evolution (Slater and Pennell 2013). We would expect these MDI values to be higher than those calculated against the BM simulations, as we expect calcar length evolution to more closely emulate an EB pattern of disparification than a BM pattern.

CT SCANNING

To examine calcar anatomy in the context of other ankle and foot bones across bat species, we dissected and μCT scanned one foot each of 19 fluid-preserved bat specimens representing 13 families within Chiroptera. We also μCT scanned three whole (nondissected) fluid-preserved specimens representing three additional bat families (Appendix S1) for a total sample of 22 species representing 16 families. These specimens were sourced from museum collections, research collections in the Santana Lab and the Herring Lab at the University of Washington, and the Lubee Bat Conservancy. We segmented (digitally dissected) the tarsals, the calcar, and other accessory ossicles in each μCT scan using Mimics version 19 (Materialise, Ann Arbor, MI, USA). The resulting 3D renderings allowed us to compare tarsal osteology across our samples in unprecedented detail.

Previous studies of pteropodid calcar anatomy describe a calcar that inserts on the tendon of the gastrocnemius muscle. This tendon then inserts on the calcaneal tuberosity. In contrast, calcars of the other bat families articulate directly with the calcaneus; thus, it has been hypothesized that pteropodid calcars are not homologous to the calcars of other bats (Schutt and Simmons 1998). In previous phylogenetic hypotheses, Pteropodidae was considered the sister clade to all of the other bat families, which were collectively referred to as the "Microchiroptera." However, after the phylogeny of Chiroptera was revised using molecular data, nonpteropodid bats were rendered paraphyletic (Teeling et al. 2005). As a consequence, the hypothesis of a lack of homology between the pteropodid calcar and the calcar of the "microbats" became a less parsimonious explanation than that of a homologous calcar across Chiroptera. To better assess the soft tissue morphology of the calcars in the Pteropodidae, we used diceCT (Gignac et al. 2016) and conventional μCT scanning to image the feet of the three pteropodid species in our sample. For diceCT scanning, we placed each fluid-preserved specimen in a solution of Lugol's iodine (3% total solute) for two to three days prior to CT scanning. The iodine solution increases the x-ray opacity of soft tissue—particularly muscle—in the sample, allowing for the visualization of this tissue in the μCT scan. Then, we dissected each of the pteropodid feet to further assess the connection between the calcar spur and the calcaneus. A list of scanned specimens and μCT scanner settings is provided in Appendix S1.

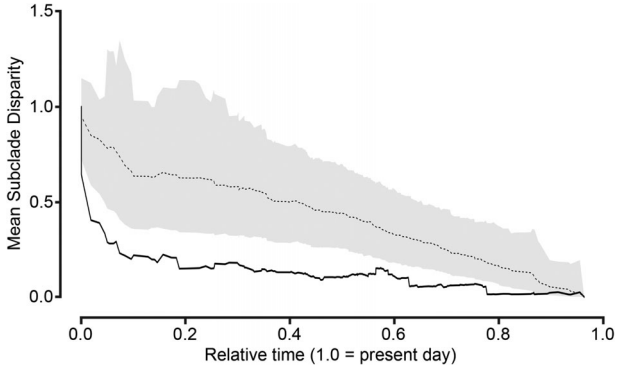

Figure 3. A disparity-through-time analysis supports an early burst of calcar length evolution. The black line indicates the mean subclade disparity through time for the measured calcar-to-tibia length ratios, the dotted line is the mean subclade disparity through time for 1000 Brownian motion simulations, and the gray band indicates a 95% confidence range for the simulations.

HISTOLOGY

We used both the μCT scans and histological sections of the dissected specimens to compare calcar tissue composition across 18 bat species (Appendix S1). Calcified calcar samples were first decalcified in 14% EDTA aqueous solution neutralized with ammonium hydroxide. Because we had difficultly completely decalcifying some samples in EDTA, we transferred them to 5% aqueous formic acid for further decalcification. We then dehydrated, cleared, and embedded all samples in paraffin wax. We sectioned each paraffin block at 5–8 μm with a Leica RM2145 microtome, mounted the sections to slides, then cleared, rehydrated, and stained the sections using either modified Mayer's hematoxylin and Mallory's triple connective tissue stain (Humason 1962) or Weigert's iron hematoxylin and fast green/safranin O. For all samples, we determined calcar tissue composition by cell and substrate morphology, not by stain color. We imaged the sections with a Nikon Eclipse E600FN compound microscope and an AmScope MU300 camera.

Table 1. Results from evolutionary model comparisons.

	Model	σ^2	z_0	a	w_{AICc}	ΔAIC_c
Calcar/Tibia						
All data	BM	0.0011	0.7073	–	<0.001	23.579
	EB	**0.0056**	**0.6872**	**−0.0434**	**>0.999**	**0**
No zero lengths	BM	0.0010	0.7568	–	<0.001	16.167
	EB	**0.0041**	**0.7524**	**−0.0374**	**>0.999**	**0**
No zero lengths or Pteropodidae	BM	0.0010	0.8348	–	0.0477	5.952
	EB	0.0034	0.8313	–0.0299	0.9353	0
Calcar/Forearm						
All data	BM	0.0002	0.2854	–	<0.001	22.207
	EB	**0.0008**	**0.2787**	**−0.0416**	**>0.999**	**0**
No zero lengths	BM	0.0001	0.3055	–	0.0009	13.962
	EB	**0.0005**	**0.3053**	**−0.0345**	**0.9987**	**0**
No zero lengths or Pteropodidae	BM	0.0002	0.3373	–	0.1415	3.485
	EB	0.0004	0.3374	–0.0252	0.8081	0
Calcar/Tibia						
All Data	BM	0.4344	0.0	–	<0.001	20.036
	EB	**2.1063**	**−0.3221**	**−0.0412**	**>0.999**	**0**
No Zero lengths	BM	0.3899	0.0	–	0.0007	14.395
	EB	**1.6065**	**−0.0694**	**−0.0365**	**0.9990**	**0**
No Zero lengths or Pteropodidae	BM	0.3491	0.0	–	0.1577	3.212
	EB	0.8923	–0.0675	–0.0234	0.7861	0
Calcar/Forearm						
All data	BM	0.4489	0.0	–	<0.001	16.869
	EB	**1.9658**	**−0.2503**	**−0.0383**	**>0.999**	**0**
No zero lengths	BM	0.4092	0.0	–	0.0038	11.149
	EB	**1.4769**	**−0.0112**	**−0.0328**	**0.9949**	**0**
No zero lengths or Pteropodidae	BM	0.3763	0.0	–	0.3999	0.270
	EB	0.7381	0.0004	−0.0165	0.4577	0

Calcar/Tibia and Calcar/Forearm indicate models considering ratios of calcar length to tibia and forearm length, respectively; Calcar/Tibia and Calcar/Forearm indicate models using residuals of phylogenetic regressions of the same variables.

BM, Brownian motion model; EB, early burst model; a, σ2, and z0 are the fit parameters of those models corresponding to the names used in the "fitContinuous" function (see Material and Methods); wAICc, AICc weights.

All OU models collapsed to BM models, so only BM and EB results are shown. Bold text emphasizes models with wAICc > 0.99.

Results

The calcar exhibits extensive anatomical diversity across Chiroptera. Calcars range from not externally visible (a length of zero) to considerably longer than the tibia (Fig. 2). We found strong support ($w_{AICc} > 0.99$) for the EB model of morphological evolution for calcar length relative to tibia length in all model comparisons that included pteropodid bats in the sample (Table 1). All OU models collapsed to BM models, so only model results for BM and EB models are shown. Support for the EB model decreased for the sample that did not include Pteropodidae, but our diceCT and dissection-based anatomical observations suggest that the calcars of pteropodid bats vary morphologically, and some variants resemble the morphologies of the nonpteropodid bats (see detailed anatomical descriptions below). Thus, inclusion of the Pteropodidae in these phylogenetic analyses is justified. Disparity-through-time analyses supported early diversification of calcar length in all cases, as evidenced by significantly low MDI values when compared to a null BM distribution (Fig. 3, Table 2). MDI values consistently increased when the calcar length disparity-through-time curve was compared to a distribution generated under an EB model of evolution.

Detailed investigation of calcar anatomy with μCT scans revealed that bat ankles exhibit numerous tarsal modifications and collectively contain multiple accessory ossicles (Fig. 4; descriptions in Appendix S1). However, none of these osteological modifications refute the status of the calcar as a neomorphic skeletal structure or morphological novelty. In no bat species is the calcar contiguous with another tarsal, nor is the calcar an obviously

Table 2. Results from disparity-through-time analyses.

	MDI (BM)	MDI (EB)
Calcar/Tibia		
All data	−0.284 ($P < 0.001$)	−0.105 ($P = 0.034$)
No zero lengths	−0.275 ($P < 0.001$)	−0.119 ($P = 0.036$)
No zero lengths or Pteropodidae	−0.236 ($P = 0.002$)	−0.112 ($P = 0.063$)
Calcar/Forearm		
All data	−0.287 ($P < 0.001$)	−0.113 ($P = 0.023$)
No zero lengths	−0.278 ($P < 0.001$)	−0.125 ($P = 0.013$)
No zero lengths or Pteropodidae	−0.223 ($P = 0.001$)	−0.113 ($P = 0.065$)
Calcar/Tibia		
All data	−0.223 ($P < 0.001$)	−0.056 ($P = 0.182$)
No zero lengths	−0.221 ($P = 0.001$)	−0.066 ($P = 0.161$)
No zero lengths or Pteropodidae	−0.195 ($P = 0.003$)	−0.0898 (p = 0.108)
Calcar/Forearm		
All data	−0.222 ($P = 0.001$)	−0.055 ($P = 0.195$)
No zero lengths	−0.207 ($P = 0.004$)	−0.075 ($P = 0.128$)
No zero lengths or Pteropodidae	−0.170 ($P = 0.027$)	−0.093 ($P = 0.129$)

MDI, morphological disparity index; BM, Brownian motion model; EB, early burst model.

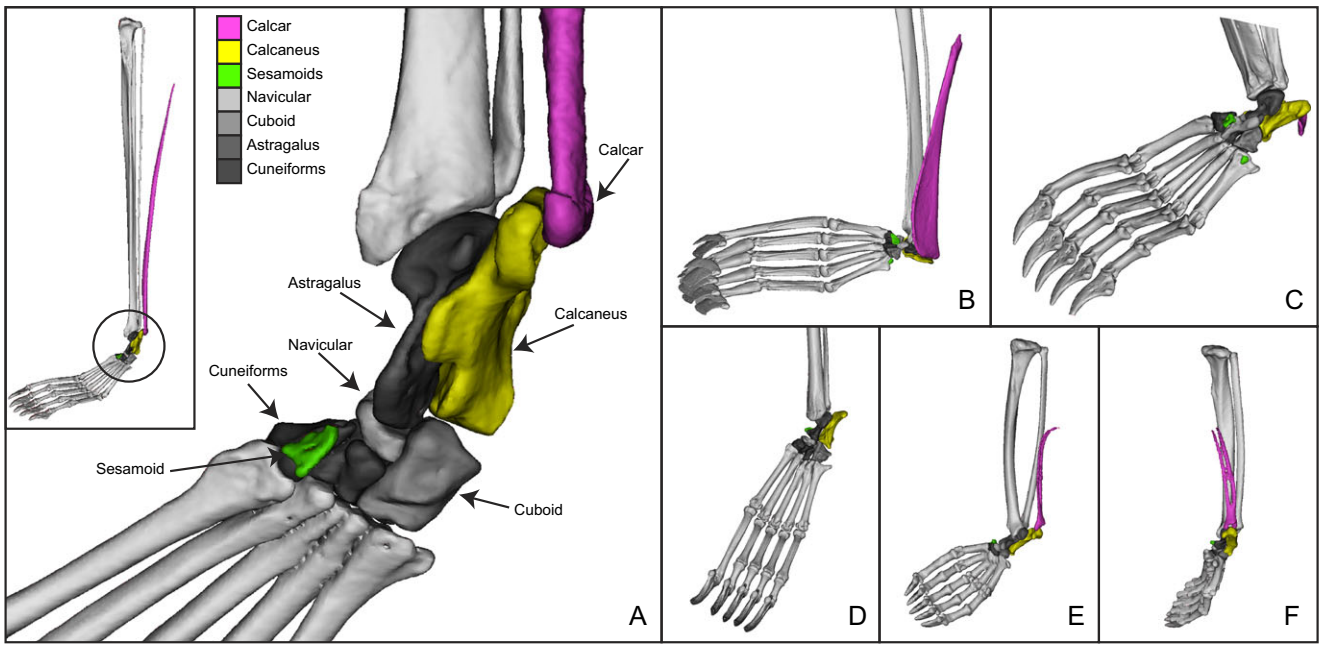

Figure 4. Bat ankle morphologies as demonstrated by rendered μCT scans. (A) Ankle of *Balantiopteryx plicata* (Santana Lab 0229-06), demonstrating calcar-calcaneus articulation (in pink-yellow), the other typical mammalian tarsals (in addition to the calcaneus; in shades of gray), and an additional sesamoid (in green). Inset demonstrates the ankle position relative to the full leg. Other bat feet μCT scans pictured are (B) *Noctilio leporinus* (FHA 1651), (C) *Desmodus rotundus* (Santana Lab 022714-06), (D) *Rhinolophus affinis* (AMNH 234034; calcar not visible due to lack of calcification), (E and F) *Mystacina tuberculata* (MVZ 173918). All are pictured in plantar view except (F), which is medial to show calcified tines on calcar.

repeated skeletal element. The calcar of any one bat species is only anatomically similar in both structure and location to calcars of other bats and not to another tarsal element.

Histological sections complemented the μCT scans in revealing tissue-level diversity in bat calcars. Although calcars are predominantly composed of uncalcified or calcified cartilage, some calcars contain ossified tissue (Fig. 5; Appendix S1). The

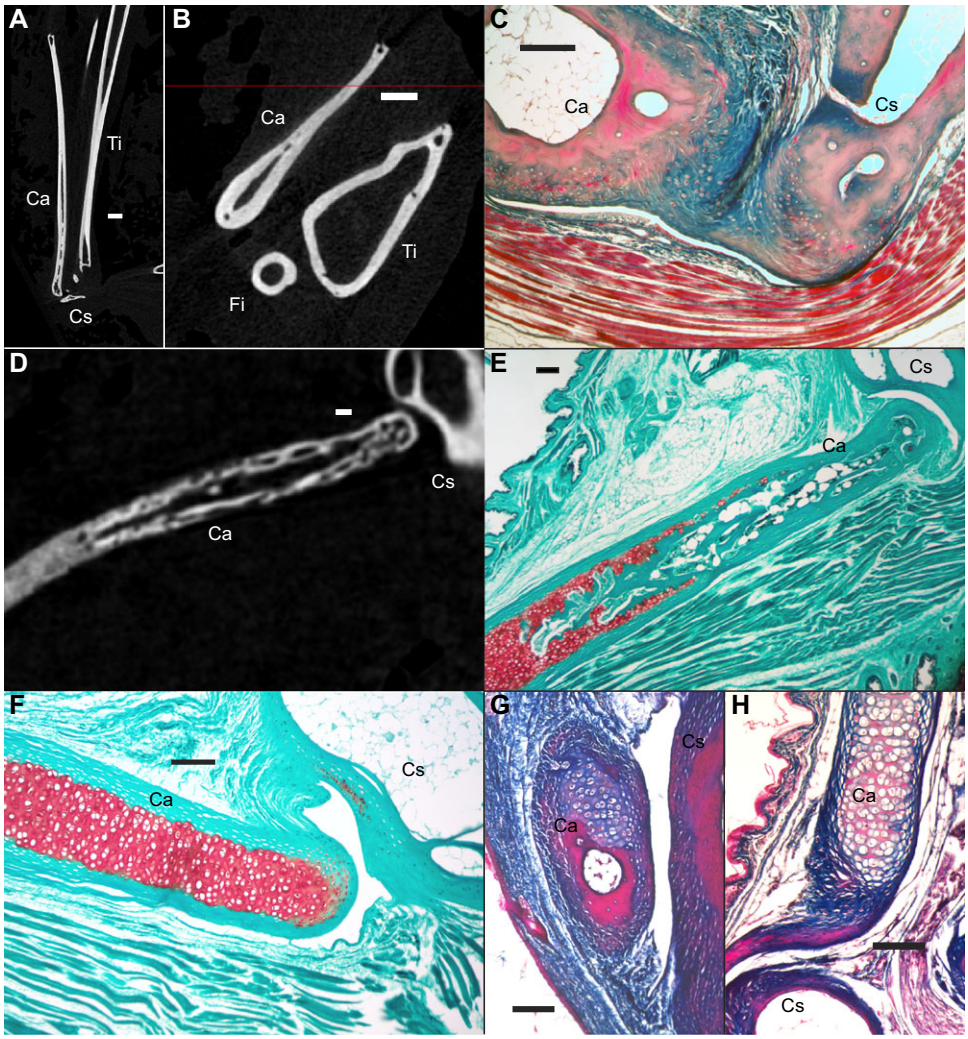

Figure 5. Histological diversity in the bat calcar. (A) Slice of μCT scan through the longitudinal axis of the calcar of *Noctilio leporinus* (FHA 1651). (B) Axial μCT scan slice through the hindlimb of *N. leporinus*, demonstrating cross-sectional shapes of the calcar and leg bones. (C) Mallory-stained histological section through the ankle of *N. leporinus*, demonstrating bony calcar tissue and a ligamentous connection between the calcar and calcaneus. (D) Slice of μCT scan and (E) fast green/safranin O-stained histological section through the longitudinal axis of the calcar of *Molossus molossus* (FHA 1857), demonstrating bony tissue in the calcar near the synovial joint with the calcaneus, which then transitions distally to calcified cartilage. (F) Fast green/safranin O-stained histological section of *Eptesicus fuscus*, showing a fully cartilaginous calcar and a synovial joint between the calcaneus and the calcar. (G) Mallory-stained histological section of *Desmodus rotundus* (Santana Lab 022714-06), demonstrating bony nodule of calcar near the synovial articulation with the calcaneus. (H) Mallory-stained histological section demonstrating calcar presence in *Rhinopoma hardwickii* (FMNH 123185). Ca, calcar; Cs, calcaneus; Fi, fibula; Ti = tibia. In all sections, the scale bar indicates 100 μm, except for (a) and (b) where it is 500 μm.

calcar of *Noctilio leporinus* (Noctilionidae; FHA 1651) is composed of thick cortical bone in the section proximal to the ankle, and both μCT scans and histological sections demonstrated the formation of trabeculae (Fig. 5A–C). The type of connective tissue also varies within a single calcar, along a continuum of cartilage, calcified cartilage, and bone. The calcar of *Molossus molossus* (Molossidae; FHA 1857) is bony proximately and cartilaginous distally; as the bone grades into cartilage, only the interior of the calcar shaft is bony, and this bony tissue is surrounded by a thick layer of tissue that appears more cartilage-like (Fig. 5D, E). This partially bony calcar contrasts with the typical cartilaginous calcar of other species, as exemplified by the primarily calcified cartilage calcar of *Eptesicus fuscus* (Vespertilionidae; Santana Lab KES 037; Fig. 5F). Both the *E. fuscus* and *M. molossus* calcars are surrounded by a thick, perichondrium-like envelope (Fig. 5E and 5F, respectively). *Pteronotus quadridens* (Mormoopidae; FHA 780) and *Macrotus waterhousii* (Phyllostomidae; FHA 135) also have bony proximal ends of their calcars, but the

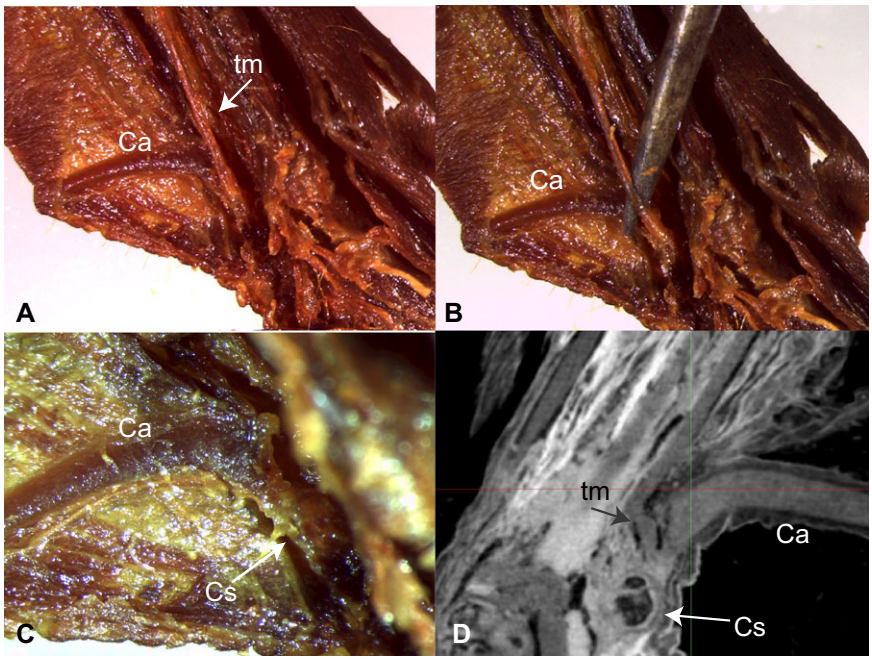

Figure 6. Photographs of dissection of the *Cynopterus brachyotis* (UWBM 82863) ankle, demonstrating separation between the calcar and the tendon of the gastrocnemius muscle. (a)–(c) are dissection photos of an iodine-stained specimen. (b) Pin demonstrates the separation between the calcar and the tendon. (c) shows the insertion of the calcar on the calcaneal tuberosity after the tendon has been dissected out. (d) is a slice of the diceCT scan demonstrating the separation between the calcar and the tendon and their two distinct insertions on the calcaneus. Ca, calcar; Cs, calcaneus; tm, tendon of the gastrocnemius muscle.

degree to which this ossification extends distally varies between the two species (Appendix S1). The short calcar of *Desmodus rotundus* (Phyllostomidae; Santana Lab 022714-06) also exhibits bony tissue (Fig. 5G).

Histological sections also confirmed the presence of a synovial joint between the calcar and the calcaneus in several bat species (Fig. 5E–G; Appendix S1) and the presence of a relatively small, uncalcified, cartilaginous calcar in one species in which the calcar was thought to be absent (*Rhinopoma hardwickii*, Rhinopomatidae; FMNH 123185; Fig. 5H). Our anatomical analyses also highlighted known shape differences across bat calcars; although most calcars take the form of a rod with an approximately elliptical cross-section, some exhibit notably divergent shapes. For example, a cartilaginous hook-like "keel" structure protrudes from the main shaft of the calcar in some species, including *Eptesicus fuscus*, *Myotis californicus* (Vespertilionidae; Santana Lab KES 026), and *Thyroptera tricolor* (Thyropteridae; MVZ 158246). The bony portion of the calcar of *Noctilio leporinus* exhibits an antero-posteriorly flattened cross-section with multiple cavities in the bony tissue (Fig. 5B). We describe, for the first time, that the calcar of *Mystacina tuberculata* (Mystacinidae; MVZ 173918) has two distinct calcified tines (Fig. 4E, F), a unique morphology among the calcars in our sample.

The diceCT scans and dissections of pteropodid feet revealed calcar anatomical diversity within the Pteropodidae. The diceCT scan of *Cynopterus brachyotis* (Pteropodidae; UWBM 82863) indicates that the calcar and the tendon of the gastrocnemius muscle make two separate, distinct insertions on the calcaneal tuberosity. We confirmed this observation through a dissection in which we were able to cleanly pass a pin between the insertions of the calcar and the tendon on the calcaneus (Fig. 6). However, dissections of the calcars of *Rousettus aegyptiacus* (Herring Lab 224) and *Pteropus* sp. (Herring Lab 76) indicated that the calcar tissue is contiguous with the tendon of the gastrocnemius muscle. DiceCT scans of these species were inconclusive, as iodine solution only slightly increases CT scan image contrast in cartilage. More detailed anatomical descriptions of each species examined with μCT scanning and histological sectioning are provided in Appendix S1.

Discussion

The bat calcar is a skeletal novelty that has anatomically diversified widely throughout Chiroptera. This diversification appears to have occurred early in chiropteran history, as evidenced by support for an early burst model of calcar length evolution and the corresponding negative morphological disparity indices. This is consistent with evidence for early diversification of bats in the fossil record (Smith et al. 2012) and an overall declining rate of speciation in Chiroptera (Shi and Rabosky 2015). Specimens

referred to the Onychonycteridae, one of the earliest bat families, have been found on both the North American and Eurasian Eocene landmasses (Hand et al. 2015). By the end of the Eocene, bats are known from six continental land masses (Smith et al. 2012; Hand et al. 2015). Eocene bat postcrania are best preserved in the Green River Formation of WY, USA and the famous Messel Lagerstätten near Messel, Germany. *Onychonycteris finneyi*, which represents the earliest known record of a calcar, also had intermediate postcranial characteristics, with limb proportions between those of bats and nonvolant mammals (Simmons et al. 2008). However, no calcars have been found in postcranial fossils of *Icaronycteris index*, another Green River bat like *O. finneyi*, but with limb proportions typical of some extant bats. Among the Messel bats, *Hassianycteris*, *Palaeochiropteryx*, and *Tachypteron* had calcars, but no calcars have been reported in specimens of *Archaeonycteris* (Simmons and Geisler 1998; Storch et al. 2002). Additionally, no evidence of an articulation facet has been found on the calcanei of *Icaronycteris* and *Archaeonycteris* (Simmons and Geisler 1998). Because calcars vary in amount of calcification, it is possible that uncalcified cartilage calcars were not preserved in these taxa; nonetheless, it is clear that Eocene bats exhibited diversity in either the presence of a calcar or in the amount of calcar calcification soon after the first bats evolved flight.

We found weaker support for the EB model when only nonpteropodid calcars were included in the analyses. However, our pteropodid diceCT scan and dissection results call into question the proposition that the pteropodid calcar is not homologous to the calcar of other bats. We have demonstrated that the calcar morphology of at least one pteropodid individual (*Cynopterus brachyotis*) differs from the calcar morphology of other pteropodids; its relation to the surrounding connective tissue makes it more similar to the "microbat" calcar condition. This intermediate anatomical condition in *C. brachyotis* suggests that it is more appropriate to consider the calcars of all bats in macroevolutionary analyses, rather than just those of the paraphyletic "microchiroptera."

Support for the EB model of morphological evolution is notoriously low in the macroevolution literature (Harmon et al. 2010). It has been proposed that this could be an artefact of either hypothesis testing at too low of a taxonomic level, such that the signal of the "early burst" of the higher level clade has been lost, or a consequence of testing variables that are not functionally linked to the specific radiation, such as body mass and overall shape (Slater and Friscia, 2019). The evolution of wings in the early Chiroptera is a type of extensive morphological change that would be expected to precede a burst of diversification, as flight would allow access to an entirely new ecospace (other examples summarized in Erwin 2015). The calcar abruptly appeared in the fossil record as part of this wing structure and is now found in the vast majority of bats. When we tested an early burst hypothesis of calcar evolution across all of Chiroptera, we found that the calcar—a distinct synapomorphy associated with an aerial ecological mode—retains the signal of an early diversification burst. The true key innovation, however, is likely the full wing apparatus, which not only includes the novel calcar but also the elongation of the forelimb bones and the evolution of novel and developmentally retained wing membranes.

Across extant bats, the calcar exhibits interspecific diversity in anatomical parameters that are likely to affect function, both in terms of overall structure (e.g., length and shape) and material (histological) composition. Although others have noted differences in the amount of calcar calcification among species based on dissection observations and clearing and staining procedures (Schutt and Simmons 1998; Koyabu and Son 2014; Reyes-Amaya et al. 2017), this is the first study to histologically confirm the presence of ossified tissue in the bat calcar. Given that there is extensive variation in material properties between cartilage, calcified cartilage, and bone (Currey 2002), interspecific variation in calcar tissue composition, length, and/or shape would result in interspecific differences in responses to applied loading (e.g., muscular contraction or resistance of a stretched membrane). Additionally, the presence of a synovial joint between the calcar and the calcaneus, in combination with the presence of skeletal muscles that insert on the calcar (Glass and Gannon 1994; Schutt and Simmons 1998; Stanchak and Santana 2018), suggests a kinematic functional role for the calcar. Although there are reported observations of moving calcars (e.g., in *Noctilio leporinus* as they trawl bodies of water for fish prey; Vaughan 1970; Altenbach 1989), calcar motion has not yet been confirmed with a rigorous kinematic analysis in any bat species. Further detailed, quantitative analyses of calcar biomechanics, including material testing and behavioral experiments, are required to estimate the magnitude of the effect of anatomical variation on any potential calcar function.

The developmental origin of the calcar is still a mystery. Although the immediate ancestry of the chiropteran lineage is unknown (Halliday et al. 2017), no calcar-like structure is found in earlier eutherian mammals. However, the discovery of a calcar in a Mesozoic mammaliaform (Meng et al. 2017) raises the possibility of a deep homological explanation for the origin of the calcar (Shubin et al. 2009). One hypothesis for calcar development is that it initially develops within existing connective tissue in the hindlimb membrane via a process of metaplasia (Carter and Beaupré 2007). The condition of the pteropodid calcar, as described here, may provide incremental support for this hypothesis. Connective tissue (cartilage, tendon, and even bone) is both plastic and labile (Hall 2015). The calcar may have arisen in a mass of connective tissue in close proximity to the calcaneus, perhaps as that mass of tissue was placed under stress during

the development of the hindlimb membrane. Consequently, differences among species in the association of the calcar with the calcaneus may be the result of relatively minor developmental alterations. Our finding of many sesamoids in bat feet, consistent with a recent assessment of bat sesamoids (Amador et al. 2018), suggests a propensity for metaplastic cartilage and bone development in bat feet, as tendon metaplasia is hypothesized to play a role in sesamoid development (Sarin et al. 1999; but see also Eyal et al. 2015, 2019). Developmental plasticity may also lead to intraspecific variation in calcar anatomy or even presence. This might be a fruitful path of further study in light of our finding of a small, calcar-like structure in the foot of one specimen of *Rhinopoma hardwickii*.

The skeletal ossicles associated with skin membranes of mammals are under-explored in studies of morphological evolution (Vickaryous and Olson 2007). The bat calcar is an anatomically diverse skeletal novelty found in a vast majority of species of a highly diverse clade of mammals. It evolved into a potentially functionally important part of the bat wing, morphologically diversifying during the early radiation of bats, which lends support to the idea that evolutionary novelty can, in some cases, precede and prompt adaptive radiations. Additional, focused studies of the bat calcar—especially of its function and development—have a high potential to yield new knowledge of skeletal biology and a better understanding of the mechanisms through which the skeleton evolves into novel forms.

AUTHOR CONTRIBUTIONS

KES and SES conceived of the project. KES collected and analyzed data. KES, JHA, and SES interpreted the data analysis and wrote the paper.

ACKNOWLEDGMENTS

We thank the Division of Mammals at the Smithsonian National Museum of Natural History, the Department of Mammalogy at the American Museum of Natural History, the Mammal Collection at the Museum of Vertebrate Zoology, the Slater Museum of Natural History, the Mammal Collection at the Field Museum of Natural History, the Herring Lab at the University of Washington, and the Lubee Bat Conservancy for providing access to specimens. L. Leiser-Miller collected several specimens used in this study. O. Okoloko helped with CT scans. L. Zeman, E. Martin, and members of the Herring Lab advised on histological technique, and A.P. Summers provided use of the μCT scanner at Friday Harbor Laboratories. The project benefited from discussion with participants of the 2015 and 2018 Annual Meetings of the North American Society for Bat Research. A.A. Curtis, Z.A. Kaliszewska, R.M. Kelly, and L. Leiser-Miller provided advice on several manuscript drafts. KES was funded by a National Science Foundation (NSF) Doctoral Dissertation Improvement Grant (#1700845), a Theodore Roosevelt Memorial Grant from the American Museum of Natural History, a Grant-in-Aid of Research from the American Society of Mammalogists, the Iuvo Award from the University of Washington Department of Biology, and funds from the Department of Mammalogy at the Burke Museum of Natural History and Culture. SES and JHA were funded by NSF Grant #1557125.

DATA ARCHIVING

CT scans will be uploaded to Morphosource upon acceptance and available at time of publication or available from the corresponding author. Data sets and code will be provided in a Dryad respository, under number https://doi.org/10.5061/dryad.qv10c62. Anatomical descriptions will be provided as Supplementary Information associated with the manuscript.

LITERATURE CITED

Adams, R. A., and K. M. Thibault. 1999. Growth, development, and histology of the calcar in the little brown bat, Myotis lucifugus (Vespertilionidae). Acta Chiropterol. 1:215–221.

Altenbach, J. S. 1989. Prey capture by the fishing bats Noctilio leporinus and Myotis vivesi. J. Mammal. 70:421–424.

Amador, L. I., N. P. Giannini, N. B. Simmons, and V. Abdala. 2018. Morphology and evolution of sesamoid elements in bats (Mammalia: Chiroptera). Am. Mus. Nov. 3905:1–40.

Bennett, S. C. 2007. Articulation and function of the pteroid bone of pterosaurs. J. Vertebr. Paleontol. 27:881–891.

Berry, R. J. 1985. Natura non facit saltum. Biol. J. Linn. Soc. 26:301–305.

Blomberg, S. P., T. Garland Jr., and A. R. Ives. 2003. Testing for phylogenetic signal in comparative data: behavioral traits are more labile. Evolution 57:717–745.

Butler, M. A., and A. A. King. 2004. Phylogenetic comparative analysis: a modeling approach for adaptive evolution. Am. Nat. 164:683–695.

Carter, D. R., and G. S. Beaupré. 2007. Skeletal function and form: mechanobiology of skeletal development, aging, and regeneration. Cambridge Univ. Press, Cambridge, U.K.

Cohn, M. J., and C. Tickle. 1999. Developmental basis of limblessness and axial patterning in snakes. Nature 399:474–479.

Coster, P., K. C. Beard, M. J. Salem, Y. Chaimanee, and J. J. Jaeger. 2015. New fossils from the Paleogene of central Libya illuminate the evolutionary history of endemic African anomaluroid rodents. Front. Earth Sci. 3:56.

Currey, J. D. 2002. Bones: structure and mechanics. Princeton Univ. Press, Princeton, NJ.

Czech, N. U., G. Klauer, G. Dehnhardt, and B. M. Siemers. 2008. Fringe for foraging? Histology of the bristle-like hairs on the tail membrane of the gleaning bat, Myotis nattereri. Acta Chiropterol. 10:303–311.

Darwin, C. 1859. On the origin of species by means of natural selection. J. Murray, London, U.K.

Darwin, C., and J. T. Costa. 2009. The annotated origin: a facsimile of the first edition of on the origin of species. Harvard Univ. Press, Cambridge, MA.

Di- Poï, N., and M. C. Milinkovitch. 2016. The anatomical placode in reptile scale morphogenesis indicates shared ancestry among skin appendages in amniotes. Sci. Adv. 2:e1600708.

Erwin, D. H. 2015. Novelty and innovation in the history of life. Curr. Biol. 25:930-940.

Eyal, S., E. Blitz, Y. Shwartz, H. Akiyama, R. Schweitzer, and E. Zelzer. 2015. On the development of the patella. Development 142:1831–1839.

Eyal, S., S. Rubin, S. Krief, L. Levin, and E. Zelzer. 2019. Common cellular origin and diverging developmental programs for different sesamoid bones. Development 146:dev167452.

Felsenstein, J. 1973. Maximum likelihood estimation of evolutionary trees from continuous characters. Am. J. Hum. Genet. 25:471–492.

———. 1985. Phylogenies and the comparative method. Am. Nat. 125:1–15.

Fenton, M. B., and W. Bogdanowicz. 2002. Relationships between external morphology and foraging behavior: bats in the genus Myotis. Can. J. Zool. 80:1004–1013.

Fenton, M. B., and N. B. Simmons. 2015. Bats: a world of science and mystery. University of Chicago Press, Chicago, IL.

Gignac, P. M., N. J. Kley, J. A. Clarke, M. W. Colbert, A. C. Morhardt, D. Cerio, I. N. Cost, P. G. Cox, J. D. Daza, C. M. Early, et al. 2016. Diffusible iodine-based contrast-enhanced computed tomography (diceCT): an emerging tool for rapid, high-resolution, 3-D imaging of metazoan soft tissues. J. Anat. 228:889–909.

Glass, P. J., and W. L. Gannon. 1994. Description of M. uropataginalis (a new muscle), with additional comments from a microscopy study of the uropatagium of the fringed myotis (Myotis thysanodes). Can. J. Zool. 72:1752–1754.

Hall, B. K. 2015. Bones and cartilage. Academic Press, Cambridge, MA.

Halliday, T. J. D., P. Upchurch, and A. Goswami. 2017. Resolving the relationships of Paleocene placental mammals. Biol. Rev. 92:521–550.

Hand, S. J., B. Sigé, M. Archer, G. F. Gunnell, and N. B. Simmons. 2015. A new early Eocene (Ypresian) bat from Pourcy, Paris Basin, France, with comments on patterns of diversity in the earliest chiropterans. J. Mamm. Evol. 22:343–354.

Hansen, T. F. 1997. Stabilizing selection and the comparative analysis of adaptation. Evolution 51:1341–1351.

Harmon, L. J., J. A. Schulte, J. B. Losos, and A. Larson. 2003. Tempo and mode of evolutionary radiation in igunaian lizards. Science 301:961–964.

Harmon, L. J., J. T. Weir, C. D. Brock, R. E. Glor, and W. Challenger. 2007. GEIGER: investigating evolutionary radiations. Bioinformatics 24:129–131.

Harmon, L. J., J. B. Losos, T. Jonathan Davies, R. G. Gillespie, J. L. Gittleman, W. Bryan Jennings, K. H. Kozak, M. A. McPeek, F. Moreno-Roark, T. J. Near, et al. 2010. Early bursts of body size and shape evolution are rare in comparative data. Evolution 64:2385–2396.

Hibbeler, R. C. 2007. Mechanics of materials. Prentice Hall, Upper Saddle River, NJ.

Humason, G. L. 1962. Animal tissue techniques. W.H. Freeman and Co, New York, NY.

Huxley, T. H. 1860. Darwin on the origin of species. Westminst. Rev. 17:541–570.

Jablonski, D. 2017. Approaches to macroevolution: 1. General concepts and origin of variation. Evol. Biol. 44:427–450.

Jackson, S. M. 2012. Gliding mammals of the world. CSIRO Publishing, Clayton, Australia.

Johnson-Murray, J. L. (1987). The comparative myology of the gliding membranes of Acrobates, Petauroides and Petaurus contrasted with the cutaneous myology of Hemibelideus and Pseudocheirus (Marsupialia, Phalangeridae) and with selected gliding Rodentia (Sciuridae and Anamoluridae). Aust. J. Zool. 35:101–113.

Kawashima, T., R. W. Thorington Jr, P. W. Bohaska, and F. Sato. 2017. Evolutionary transformation of the palmaris longus muscle in flying squirrels (Pteromyini: Sciuridae): an anatomical consideration of the origin of the uniquely specialized styliform cartilage. Anat. Rec. 300:340–352.

Kobayashi, M. 2017. Homology of the muscles within the uropatagium membrane in Leschenault's rousette (Rousettus leschenaultii). Z. Saugetierkd. 86:102–106.

Koyabu, D., and N. T. Son. 2014. Patterns of postcranial ossification and sequence heterochrony in bats: Life histories and developmental trade-offs. J. Exp. Zool. Part B. 322:607–618.

Kunz, T. H. and M. B. Fenton, eds. 2005. Bat Ecology. University of Chicago Press, Chicago, IL.

López-Fernández, H., J. H. Arbour, K. O. Winemiller, and R. L. Honeycutt. 2013. Testing for ancient adaptive radiations in Neotropical cichlid fishes. Evolution 67:1321–1337.

Martill, D. M., H. Tischlinger, and N. R. Longrich. 2015. A four-legged snake from the Early Cretaceous of Gondwana. Science 349:416–419.

Meng, Q. J., D. M. Grossnickle, D. Liu, Y. G. Zhang, A. I. Neander, Q. Ji, and Z. X. Luo. 2017. New gliding mammaliaforms from the Jurassic. Nature 548:291–296.

Moczek, A. P. 2008. On the origins of novelty in development and evolution. Bioessays 30:432–447.

Müller, G. B. 2010. Epigenetic innovation. Pp. 307–332 *in* M. Pigliucci and G. B. Müller, eds. Evolution: the extended synthesis. MIT Press, Cambridge, MA.

Musser, J. M., G. P. Wagner, and R. O. Prum. 2015. Nuclear β-catenin localization supports homology of feathers, avian scutate scales, and alligator scales in early development. Evol. Dev. 17:185–194.

Novick, A., and B. A. Dale. 1971. Foraging behavior in fishing bats and their insectivorous relatives. J. Mammal. 52:817–818.

Orr, H. A., and J. A. Coyne. 1992. The genetics of adaptation: a reassessment. Am. Nat. 140:725–742.

Pennell, M. W., J. M. Eastman, G. J. Slater, J. W. Brown, J. C. Uyeda, R. G. FitzJohn, M. E. Alfaro, and L. J. Harmon. 2014. geiger v2.0: an expanded suite of methods for fitting macroevolution models to phylogenetic trees. Bioinformatics 30:2216–2218.

Peterson, T., and G. B. Müller. 2013. What is evolutionary novelty? Process versus character based definitions. Journal of Experimental Zoology Part B: Molecular and Developmental Evolution 320:345–350.

Pigliucci, M. 2008. What, if anything, is an evolutionary novelty? Philos. Sci. 75:887–898.

R Core Team. 2017. R: a language and environment for statistical computing. R foundation for statistical computing, Vienna, Austria.

Revell, L. J. 2009. Size-correction and principal components for interspecific comparative studies. Evolution 63:3258–3268.

———. 2010. Phylogenetic signal and linear regression on species data. Methods Ecol. Evol. 1:319–329.

———. 2012. phytools: An R package for phylogenetic comparative biology (and other things). Methods Ecol. Evol. 3:217–223.

———. 2013. Two new graphical methods for mapping trait evolution on phylogenies. Methods Ecol. Evol. 4:754–759.

Reyes-Amaya, N., A. Jerez, and D. Flores. 2017. Morphology and postnatal development of lower hindlimbs in Desmodus rotundus (Chiroptera: Phyllostomidae): a comparative study. Anat. Rec. 300:2150–2165.

Sarin, V. K., G. M. Erickson, N. J. Giori, A. G. Bergman, and D. R. Carter. 1999. Coincident development of sesamoid bones and clues to their evolution. Anat. Rec. 257:174–180.

Schutt, W. A., and N. B. Simmons. 1998. Morphology and homology of the chiropteran calcar, with comments on the phylogenetic relationships of Archaeopteropus. J. Mamm. Evol. 5:1–32.

Shi, J. J., and D. L. Rabosky. 2015. Speciation dynamics during the global radiation of extant bats. Evolution 69:1528–1545.

Shubin, N., C. Tabin, and S. Carroll. 2009. Deep homology and the origins of evolutionary novelty. Nature 457:818–823.

Simmons, N. B. 2005. Order Chiroptera. Pp. 312–529 *in* D. E. Wilson and D. M Reeder, eds. Mammal species of the world: a taxonomic and geographic reference. Johns Hopkins Univ. Press, Baltimore, MD.

Simmons, N. B., and J. H. Geisler. 1998. Phylogenetic relationships of Icaronycteris, Archaeonycteris, Hassianycteris, and Palaeochiropteryx to extant bat lineages, with comments on the evolution of echolocation and foraging strategies in Microchiroptera. B. Am. Mus. Nat. Hist. 235:1–182.

Simmons, N. B., K. L. Seymour, J. Habersetzer, and G. F. Gunnell. 2008. Primitive early Eocene bat from Wyoming and the evolution of flight and echolocation. Nature 451:818–821.

Simpson, G. G. 1944. Tempo and mode in evolution. Columbia Univ. Press, New York, NY.

Slater, G. J., and A. R. Friscia. 2019. Hierarchy in adaptive radiation: a case study using the Carnivora (Mammalia). Evolution 73:524–539.

Slater, G. J., and M. W. Pennell. 2013. Robust regression and posterior predictive simulation increase power to detect early bursts of trait evolution. Syst. Biol. 63:293–308.

Slater, G. J., S. A. Price, F. Santini, and M. A. Alfaro. 2010. Diversity vs disparity and the evolution of modern cetaceans. Proc. R Soc. Lond. B Biol. Sci. 277:3097–3104.

Smith, T., J. Habersetzer, N. B. Simmons, and G. F. Gunnell. 2012. Systematics and paleobiogeography of early bats. Pp. 23–66 *in* G. F. Gunnell and N. B. Simmons, eds. Evolutionary history of bats: fossils, molecules and morphology. Cambridge, Univ. Press, Cambridge, U.K.

Stanchak, K. E., and S. E. Santana. 2018. Assessment of the hindlimb membrane musculature of bats: Implications for active control of the calcar. Anat. Rec. 301:441–448.

Storch, G., B. Sigé, and J. Habersetzer. 2002. Tachypteron franzeni n. gen., n. sp., earliest emballonurid bat from the Middle Eocene of Messel (Mammalia, Chiroptera). Palaeontol. Z. 76:189–199.

Teeling, E. C., M. S. Springer, O. Madsen, P. Bates, S. J. O'brien, and W. J. Murphy. 2005. A molecular phylogeny for bats illuminates biogeography and the fossil record. Science 307:580–584.

Vaughan, T. A. 1970. The skeletal system. Pp. 98–139 *in* W. A. Wimsatt, ed. Biology of bats v1. Academic Press, New York, NY.

Vickaryous, M. K., and W. M. Olson. 2007. Sesamoids and ossicles in the appendicular skeleton. Pp. 323–341 *In* B. K. Hall, ed. Fins into limbs: evolution, development and transformation. Univ. Chicago Press, Chicago, IL.

Wagner, G. P. 2014. Homology, genes, and evolutionary innovation. Princeton Univ. Press, Princeton, NJ.

Witton, M. P. 2013. Pterosaurs: natural history, evolution, anatomy. Princeton University Press, Princeton, NJ.

Xu, X., X. Zheng, C. Sullivan, X. Wang, L. Xing, Y. Wang, X. Zhang, J. K. O'Connor, F. Zhang, and Y. Pan. 2015. A bizarre Jurassic maniraptoran theropod with preserved evidence of membranous wings. Nature 521:70–73.

Associate Editor: G. Slater
Handling Editor: Mohamed A. F. Noor

Supporting Information

Additional supporting information may be found online in the Supporting Information section at the end of the article.

Supplementary information
Supplementary information